Actomyosin Tension Exerted on the Nucleus through Nesprin-1 Connections Influences Endothelial Cell Adhesion, Migration, and Cyclic Strain-Induced Reorientation

T. J. Chancellor,[†] Jiyeon Lee,[†] Charles K. Thodeti,[‡] and Tanmay Lele[†*]

[†]Department of Chemical Engineering, University of Florida, Gainesville, Florida; and [‡]Department of Integrative Medical Sciences, NEOUCOM, Rootstown, Ohio

ABSTRACT Endothelial cell polarization and directional migration is required for angiogenesis. Polarization and motility requires not only local cytoskeletal remodeling but also the motion of intracellular organelles such as the nucleus. However, the physiological significance of nuclear positioning in the endothelial cell has remained largely unexplored. Here, we show that siRNA knockdown of nesprin-1, a protein present in the linker of nucleus to cytoskeleton complex, abolished the reorientation of endothelial cells in response to cyclic strain. Confocal imaging revealed that the nuclear height is substantially increased in nesprin-1 depleted cells, similar to myosin inhibited cells. Nesprin-1 depletion increased the number of focal adhesions and substrate traction while decreasing the speed of cell migration; however, there was no detectable change in nonmuscle myosin II activity in nesprin-1 deficient cells. Together, these results are consistent with a model in which the nucleus balances a portion of the actomyosin tension in the cell. In the absence of nesprin-1, actomyosin tension is balanced by the substrate, leading to abnormal adhesion, migration, and cyclic strain-induced reorientation.

INTRODUCTION

The formation of new blood capillaries, or angiogenesis, involves the polarization and directed migration of endothelial cells (1,2). Research on angiogenesis has primarily focused on biochemical pathways that participate in directed endothelial cell motility (3). However, motility and polarization also require the coordinated motion of intracellular organelles. In particular, positioning of the nucleus is an important part of any dynamic changes in cell morphology (4), given that it is the largest and stiffest organelle in the cell. Yet, the physiological significance of nuclear positioning in the endothelial cell has remained unexplored.

The nucleus is positioned through physical interactions with the actomyosin, microtubule and intermediate filament cytoskeleton (4). This force transfer is hypothesized to be mediated by bonds between the cytoskeleton and proteins embedded in the nuclear envelope. Recent studies suggest that lamin (5–7), SUN proteins (4,8–11), emerin (12), and nesprins (11,13–16) are key components of the mechanical linkage between the nucleus and the cytoskeleton. There is increasing evidence that these linker of nucleus and cytoskeleton (LINC) complex proteins are required for normal cell function. Lamin A/C deficient mouse embryonic fibroblasts have reduced migration speeds and are unable to polarize in wound healing assays (7). Lamin A/C deficient fibroblasts have altered mechanotransduction as measured by abnormal NF-κB-mediated, strain-induced transcription (6). Interestingly, these cells also have a softer perinuclear cytoskeleton suggesting that lamin A/C is necessary for physically connecting F-actin to the nucleus (17,18). Similarly, emerin-deficient fibroblasts have irregular nuclear shape and respond abnormally to mechanical forces (12).

Nesprin-1 and nesprin-2 are nuclear membrane proteins that bind to F-actin (19) through the N-terminus and to transmembrane SUN proteins via the C-terminus (8–11,20). These proteins are hypothesized to be part of the LINC complex (11,16,21). Nesprin-1 mislocalization in HELA and Swiss 3T3 cells results in a softer cytoplasm (18), possibly due to a decrease in F-actin linkage to the nucleus. Nesprin-1 is necessary for anchorage of muscle nuclei to the neuromuscular junction (22), as well as for positioning of nonsynaptic and synaptic nuclei in skeletal muscle (16). Disruption of nesprin-1 induces an Emery-Dreifuss dystrophy like phenotype in mice (23) and nesprin mutations are associated with the pathogenesis of Emery-Dreifuss dystrophy in humans (13).

The function of nesprin-1 in endothelial cells has received little attention. We show that nesprin-1 knockdown in endothelial cells by siRNA transfection causes a lack of cell reorientation under cyclic strain, increased cell traction and focal adhesion assembly, and decreased cell migration. An increase in nuclear height is observed in nesprin-1 depletion cells similar to blebbistatin-treated, myosin II-inhibited cells. Our results suggest a model in which the nucleus balances a part of the actomyosin tension in the cell. In the absence of nesprin-1, actomyosin tension is balanced entirely by the substrate, causing increased cell traction, decreased migration, and altered nuclear height.

MATERIALS AND METHODS

Cell culture

Human umbilical vascular endothelial cells (HUVECs) were maintained in DMEM-high glucose (Cellgro, Manassas, VA) supplemented with 10%

Submitted May 18, 2009, and accepted for publication April 1, 2010.

*Correspondence: tlele@che.ufl.edu

Editor: Jason M. Haugh.

© 2010 by the Biophysical Society

0006-3495/10/07/0115/9 $2.00

doi: 10.1016/j.bpj.2010.04.011

donor bovine serum (Cellgro) and maintained at 37°C in a humidified 5% CO_2 environment. HUVECs were tested for their endothelial function with an in vitro 3D angiogenesis assay and were found to form typical tube-like structures characteristic of endothelial cells (Fig. S1 in the Supporting Material). In wounding experiments, cells were seeded at 80% confluence on fibronectin-coated (5 μg/mL) glass bottom dishes (MatTek, Ashland, MA) cultured to confluence.

siRNA knock down of nesprin-1

Cells were transfected with 100 nM of SMARTpool siRNAs (Dharmacon, Lafayette, CO) against human nesprin-1 using siLentFect lipid transfection reagent (BioRad, Hercules, CA). The siRNA oligonucleotide target sequences used were as follows: GAAAUUGUCCCUAUUGAUU, GCAAAGCCCUGGAUGAUAG, GAAGAGACGUGGCGAUUGU and CCAAACGGCUGGUGUGAUU. Nontargeting SMARTpool siRNAs served as controls.

Western blotting

Cells cultured in regular growth media were washed with cold phosphate buffered saline (PBS) and lysed with cell lysis buffer (Cell Signal, Boston, MA) for 10 min on ice. Cells were scraped, collected, and centrifuged at 10,000 rpm for 10 min at 4°C. The supernatant was collected and sodium dodecyl sulfate (SDS) sample buffer was added and stored at −20°C until use. The samples were separated on 10% SDS polyacrylamide gels and then transferred onto a PVDF membrane. The membranes were treated with anti-nesprin-1 mouse monoclonal antibody (Abcam, Cambridge, MA) at 1:200 dilutions in 5% milk overnight at 4°C. Phosphorylated myosin levels were measured by treating membranes with a phospho-myosin antibody (Cell Signal) which recognizes myosinlight chain 2 only when dually phosphorylated at Thr-18 and Ser-19. The membranes were then washed three times in Tris-buffered saline with 0.05% Tween 20 and treated with peroxidase conjugated secondary antibody at 1:10,000 in 5% milk in Tris-buffered saline with 0.05% Tween 20. Blots were developed using SuperSignal West Pico Chemiluminescent reagent (Pierce, Rockford, IL) and exposed to X-OMAT film (Kodak).

Immunostaining

Cells were fixed with 4% paraformaldehyde (Electron Microscopy Sciences, Fort Washington, PA) for 20 min, washed with PBS (Cellgro), and then permeabilized with 0.1% Triton X-100 in 1% bovine serum albumin solution. Cells were next incubated with nesprin-1 primary monoclonal mouse antibody (Abcam) or vinculin monoclonal mouse antibody (Sigma, St. Louis, MO) at a 1:100 dilution overnight at 4°C. Samples were washed and treated with goat-anti-mouse 488 nm fluorescent secondary antibody (Calbiochem, San Diego, CA) for 1 h at room temperature. For actin staining, cells were incubated with Alexa Fluor 594 phalloidin (Invitrogen, Carlsbad, CA) for 1 h. Nuclear staining was done using Hoechst33342 diluted at 1:100 for 30 min. The samples were imaged on a Leica SP5 confocal microscope equipped with a 63× objective.

Application of mechanical strain and measurement of cell reorientation

Cells were cultured on fibronectin (5 μg/mL) coated 6-well Uniflex plates (Flexcell, Hillsborough, NC) and exposed to 10% uniaxial strain with a frequency of 0.5 Hz for 18 h using the Flexcell-4000 system (24). Cells were then fixed and stained with phalloidin (Sigma) for imaging F-actin. Images of cells were acquired as described above and the cell angle relative to the strain direction was quantified using ImageJ software. Approximately 300 cells were evaluated for each condition corresponding to six fields; 50 cells from each field.

Cell motility assay

To assess cell motility, cells were cultured on fibronectin-treated glass bottom dishes for 6 h. The dishes were transferred onto the microscope stage and imaged with a 10× phase contrast lens inside an environmental chamber maintained at 37°C and with 5% CO_2. Images were taken every 10 min for 10 h and analyzed using a MATLAB program (The MathWorks, Natlick, MA) that tracked the position of the centroid of cells in (x,y) coordinates versus time. The mean-square displacement (MSD) was calculated from the data using nonoverlapping time intervals (25). The speed of each cell was determined from the measured displacement of the centroid at 10 min. The persistence time of each cell was calculated by fitting the MSD to the persistent random walk model using nonlinear least-square regression as reported elsewhere (26). A minimum of 17 cells were measured for each condition. Images taken 8 h after passage were also used to measure cell spreading area of cells transfected with control and nesprin-1 targeting siRNA. The area of at least 12 cells was measured for each condition using Nikon Elements software (Fig. S7).

Scratch-wound assay

Confluent cells were washed and serum starved for 24 h after which a wound was created by scraping across the surface of each monolayer using a 20-gauge needle. After wounding, the cells were washed with PBS and cultured in full growth medium. Images of the cells were taken simultaneously every 30 min for 18 h on a Nikon TE2000 microscope equipped with an environmental chamber. Nikon Elements software was used to measure the area of the wound at each time interval. Only wounds with original widths between 175 μm and 225 μm were measured. To measure cell polarization, cells were serum starved for 12 h, wounded, and treated with 2-μM lysophosphatidic acid for 4 h, fixed and stained with rabbit anti-γ-tubulin antibody (Sigma) and mouse monoclonal α-tubulin antibody (Sigma). Cells with centrosomes located within 30° of a line perpendicular to the wound were considered polarized similar to the approach in (7). Angles were measured with Nikon Elements software. At least 30 cells per condition were measured.

Traction force microscopy

Fibronectin coated polyacrylamide gels (Young's modulus of 45 kPa) for traction force microscopy were prepared on glass bottom dishes (MatTek) as described previously in Polte et al. (27). Red fluorescent microspheres (0.5 μm diameter; Invitrogen) were suspended in the polyacrylamide gel before gel formation and used as fiduciary markers. Cells were plated at low concentrations (5% confluence) and incubated for 24 h at 37°C with 5% CO_2 in full growth media. Differential interference contrast and fluorescent images of isolated cells were then taken simultaneously before and after treatment with 5% SDS (Sigma) solution. Traction force analysis was carried out using the MATLAB software and methods described in Tolić-Nørrelykke et al. (28). A minimum of eight cells were measured for each condition.

Confocal imaging to determine nuclear height

Cells were fixed with 4% paraformaldehyde and nuclei and the F-actin cytoskeleton stained as described above. The samples were imaged on a Leica SP5 confocal microscope equipped with a 63× objective. Z-stacks were acquired and Leica application suite software used to measure the height of the nucleus. Each experiment was repeated 3 times ($n > 15$). Similar procedures were used for cells treated with blebbistatin ($n > 15$).

3D in vitro angiogenesis assay

A 1:20 dilution of HUVECs was taken from an 80% confluent 12-well dish and mixed with 300 μL of Matrigel using cold glass pipettes. The Matrigel solution was then placed on a glass bottom dish (MatTek) and kept in a 37°C

incubator for 1 h. After 1 h, 2 mL of growth media was added. The growth media was changed every 2 days for 2 weeks. At the end of the experiments, the gel was imaged on a Nikon TE2000 microscope equipped with a 20× lens to analyze tube formation.

Statistical analysis

All data are presented as mean ± SE. All statistical comparisons were carried out with the Student's *t*-test. Statistical significance was assumed for $p < 0.05$.

RESULTS

siRNA knock down of nesprin-1 in HUVECs

Nesprin-1 has been shown to localize to the nuclear envelope in fibroblasts, vascular smooth muscle cells, and cardiac muscle cells (11,21,29,30). Immunostaining with a specific antibody against nesprin-1 showed a similar localization to the nuclear envelope in HUVECs (Fig. 1 *A*). Western blotting analysis (Fig. 1 *B*) showed a major band at a molecular weight of ~110 kDa, with additional bands at around 75 kDa and 40 kDa, consistent with previous studies (13,21,29). Treatment with specific siRNA against nesprin-1 reduced significantly all bands in Western blots (Fig.1, *B* and *C*). However, nesprin-1 knockdown did not alter the expression levels (Fig. S2) or the localization (Fig. S3) of a closely related member of the nesprin family, nesprin-2, confirming the specificity of nesprin-1 knockdown by the siRNA transfection. Cells transfected with nesprin-1 targeting and control siRNA were next immunostained for nesprin-1. Confocal fluorescent imaging (Fig. 1 *D*) also showed that nesprin-1 expression in siRNA transfected cells was reduced significantly compared to cells expressing control siRNA and nontransfected cells. Quantification of pixel intensity of these images further confirmed that the majority of individual cells had reduced nesprin-1 expression (Fig. S4). We believe that taken together, these results show clearly that the siRNA transfection specifically knocked down nesprin-1 in HUVECs.

Nesprin-1 knockdown abolishes cyclic strain-induced HUVEC reorientation and increases focal adhesion assembly and cell traction

Next, we investigated if nesprin-1 knockdown affected endothelial cell physiology. HUVEC reorientation in response to applied uniaxial cyclic strain was examined. Control and nesprin-1 deficient HUVECs were exposed to cyclic mechanical strain (10%, 0.5 Hz) for 18 h using the FlexCell 4000 device (24). Nontransfected HUVECs oriented predominantly along a direction perpendicular to the direction of mechanical strain (Fig. 2). F-actin staining showed that stress fibers also aligned perpendicular to the direction of the strain. In contrast, knockdown of nesprin-1 abolished HUVEC reorientation in response to cyclic strain. Further, we found that cells transfected with control siRNA responded similarly to the untreated cells, establishing the specificity of the effect of nesprin-1 knockdown on strain-induced cell reorientation.

Cell reorientation under cyclic strain requires disassembly of existing focal adhesions, and the preferential stabilization of newly formed adhesions in a direction perpendicular to applied strain (31). We therefore explored if focal adhesion assembly was altered in nesprin-1 depleted cells. Cells were immunostained for vinculin and focal adhesions were imaged on a confocal fluorescence microscope. Nesprin-1 deficient cells assembled a significantly larger number of focal adhesions compared to control cells (Fig. 3, *A* and *B* and Fig. S5). F-actin was also more concentrated toward

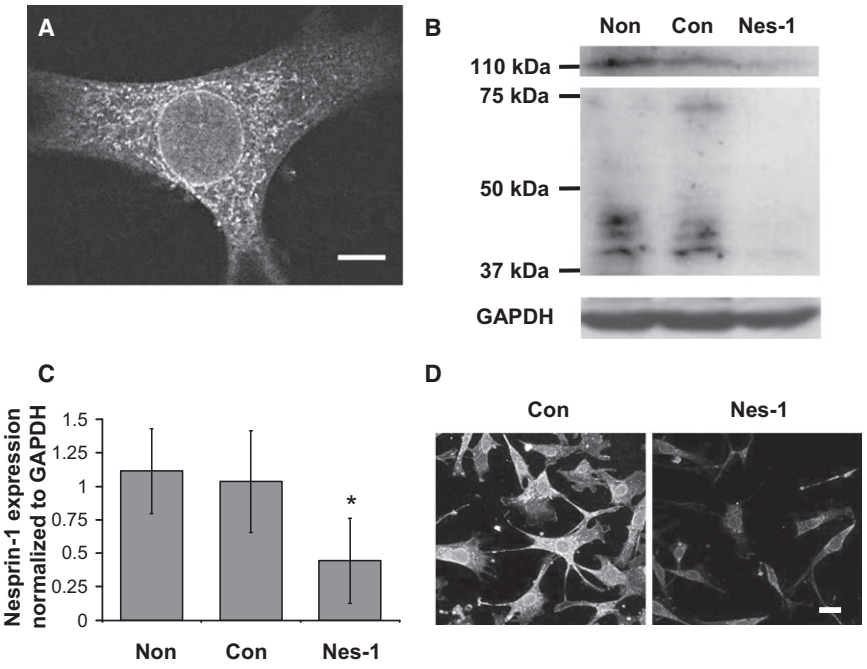

FIGURE 1 Transfection of HUVECs with siRNA targeting nesprin-1 results in a significant reduction in nesprin-1 expression. (*A*) Confocal fluorescence image of HUVEC immunostained for nesprin-1. Nesprin-1 localizes to the nuclear membrane. Scale bar = 5 μm. (*B*) Western blot analysis of nesprin-1 expression in HUVECs. HUVECs transfected with siRNA targeting nesprin-1 (Nes-1) show a significant reduction in nesprin-1 expression as compared to nontransfected cells (Non) and cells transfected with control siRNA (Con). (*C*) Quantification of nesprin-1 expression relative to GAPDH expression demonstrating a significant decrease in siRNA transfected cells. Error bars represent SE from three different experiments. *$p < .05$ (*D*) Low magnification confocal fluorescence images of HUVECs immunostained for nesprin-1. A significant reduction in nesprin-1 expression is observed in cells transfected with nesprin-1 targeting siRNA (images were acquired at the same laser power, photomultiplier gain, and magnification). Scale bar = 25 μm.

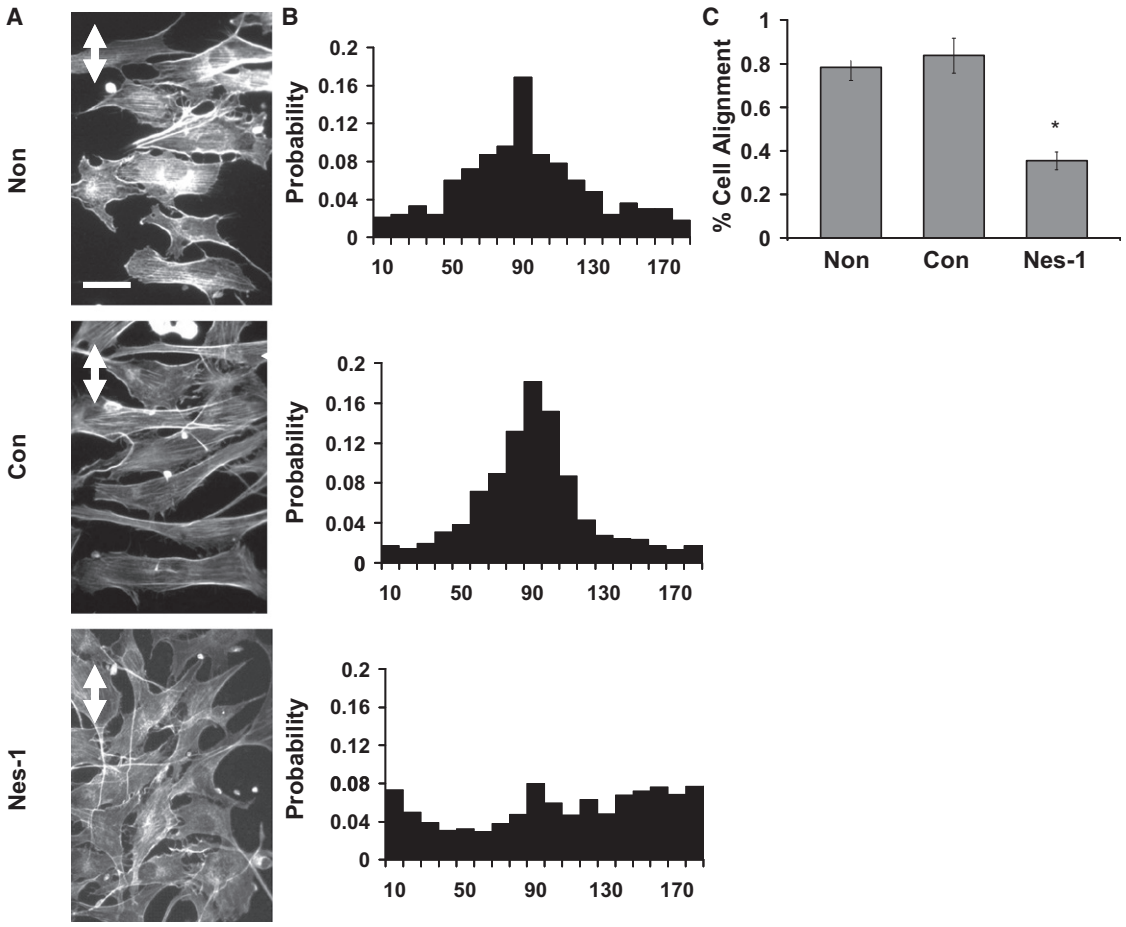

FIGURE 2 Nesprin-1 deficient HUVECs are unable to align in response to uniaxial cyclic strain. (*A*) HUVECs cultured on flexible silicon membranes coated with fibronectin were exposed to 10% cyclic, uniaxial strain at 0.5 Hz, fixed and stained with Alexa-phalloidin to visualize F-actin stress fibers. Nontransfected HUVECs and cells expressing control siRNA oriented perpendicular to the strain direction (strain direction is marked by *white double arrow*) whereas cells transfected with nesprin-1 targeting siRNA did not align in any preferred direction. Stress fibers were observed predominantly perpendicular to the strain direction except in nesprin-1 deficient cells. Scale bar = 50 μm. (*B*) Probability distributions of cell angle measured relative to strain axis. A clear preference for a direction perpendicular to the strain axis is observed in the distribution for nontransfected and control siRNA transfected cells; the distribution is random for nesprin-1 siRNA transfected cells. The distribution was quantified from pooled data from three independent experiments corresponding to 300 cells per condition. (*C*) Quantification of the reorientation response. The data is presented as percentage of cells that reoriented 90° ± 30° relative to the strain direction similar to the approach in Ghosh et al. (33). Error bars represent SE from three different experiments. *$p < 0.01$.

the base of the cell in nesprin-1 deficient cells (Fig. S6). The increased focal adhesion number suggested a potential increase in cell traction in nesprin-1 depleted cells. Using traction force microscopy, we found that nesprin-1 depletion indeed significantly increased traction stresses on the substrate (Fig. 3, *C* and *D*). Nesprin-1 deficient cells were also observed to spread more than control cells (Fig. S7).

Transient disassembly of focal adhesions restores reorientation under strain in nesprin-1 depleted cells

The above experiments motivated the hypothesis that cells were unable to reorient in response to cyclic strain owing to increased focal adhesion assembly and traction. Therefore, we reasoned that transiently causing the disassembly of focal adhesions could allow the nesprin-1 depleted cell to reorient under applied strain. To do this, we used an approach published previously to cause the time-dependent disassembly of focal adhesions by treatment with the Rho-kinase inhibitor Y27632 (32). To only cause a transient disassembly of focal adhesions, we treated the drug for a short time (30 min) after which the drug was washed off and cyclic strain was applied. Drug washout permits the reassembly of focal adhesions (33). Interestingly, cells treated in this manner were able to reorient under cyclic strain (Fig. 4). This confirms our hypothesis that nesprin-1 depleted cells are unable to reorient due to increased adhesion to the substrate.

Altered actomyosin forces on the nucleus

Actomyosin tension has been shown previously to control nuclear shape (34). The extent to which nesprin-1 mediates this force transfer to the nuclear shape is unclear. We carried

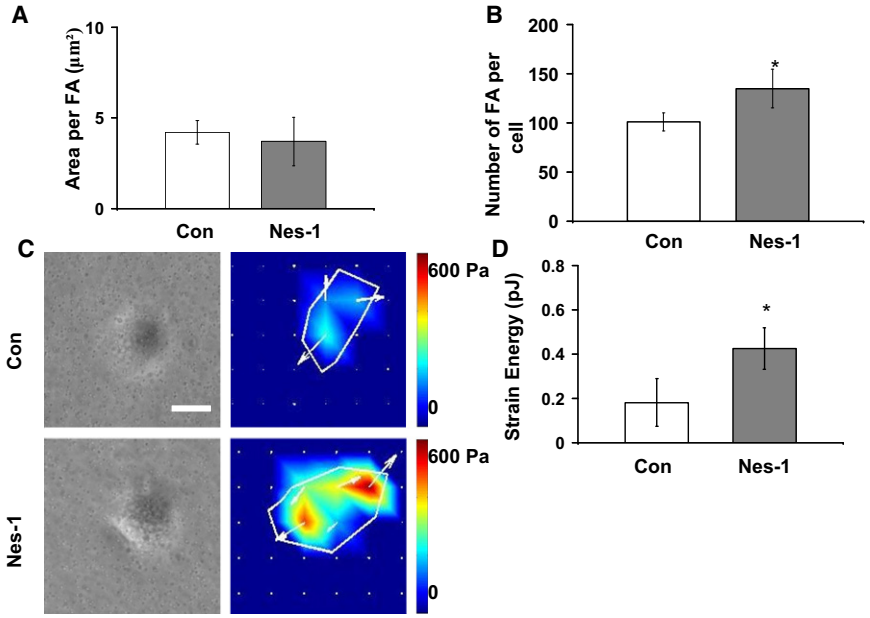

FIGURE 3 Nesprin-1 depletion results in increased cell traction and focal adhesions. (*A*) The area per FA was unchanged between cells transfected with control and nesprin-1 targeting siRNA, whereas the number of FAs (*B*) increased in nesprin-1 deficient cells ($p < 0.05$). (*C*) Representative phase contrast images and traction stress maps of cells transfected with nesprin-1 targeting and control siRNA. Scale bar = 200 μm. (*D*) Surface strain energy is increased in nesprin-1 deficient cells compared to control cells ($p < 0.05$). Error bars represent SE from three different experiments. *$p < 0.01$. A minimum of eight cells were measured for each condition.

out Z-stack imaging with a laser scanning confocal microscope of the stained nucleus in nesprin-1 deficient cells. Reconstructed 3D images were used to quantify nuclear heights. Nesprin-1 deficient cells showed a significant increase in nuclear height (7.1 $\pm$ 0.8 μm) as opposed to control cells that had nuclear heights of 5.0 $\pm$ 0.4 μm (Fig. 5, *A* and *B*). This suggests that nesprin-1 mediated pulling forces on the nucleus flatten the nucleus into a disk-like shape in endothelial cells. We next asked if inhibiting actomyosin forces could similarly change nuclear height. The nuclear heights of nontransfected cells were measured after treatment with the nonmuscle myosin II inhibitor blebbistatin (100 μM) for 1 h. A significant increase in nuclear height (6.2 $\pm$ 0.4 μm) was observed in the blebbistatin-treated cells (Fig. 5, *A* and *B*). These results support previous observations (34–36) that the nucleus balances actomyosin tension. Finally, we used the initial cell polarization assay (Fig. S8) in which rearward actomyosin motion from the leading edge of the wounded cell pushes the nucleus in a manner that gives the cell a polarized appearance (37). The nuclear-centrosomal-leading edge axis was disrupted significantly in cells, which provides further support to the conclusion that actomyosin forces are decreased significantly on the nucleus in the absence of nesprin-1.

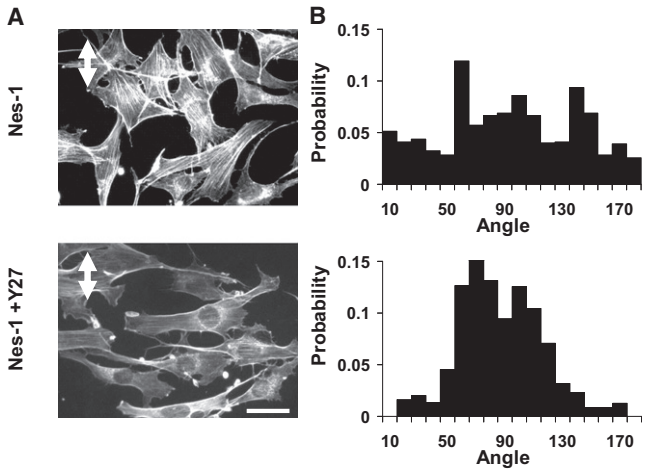

FIGURE 4 Rho kinase inhibition restores the reorientation response in nesprin-1 deficient cells. (*A*) After 18 h of 10% cyclic, uniaxial strain at 0.5 Hz (strain direction is marked by *white double arrow*), cells transfected with nesprin-1 targeting siRNA did not align in any preferred direction. Pretreatment of cells with Y27632 for 30 min followed by washout and cyclic stretching restored the reorientation response of nesprin-1 deficient cells. Scale bar = 50 μm. (*B*) Probability distributions of cell angle measured relative to strain axis. Y27632-treated nesprin-1 deficient cells have a much higher probability of reorienting perpendicular to the applied strain. The distribution was quantified from pooled data from two independent experiments corresponding to 150 cells per condition.

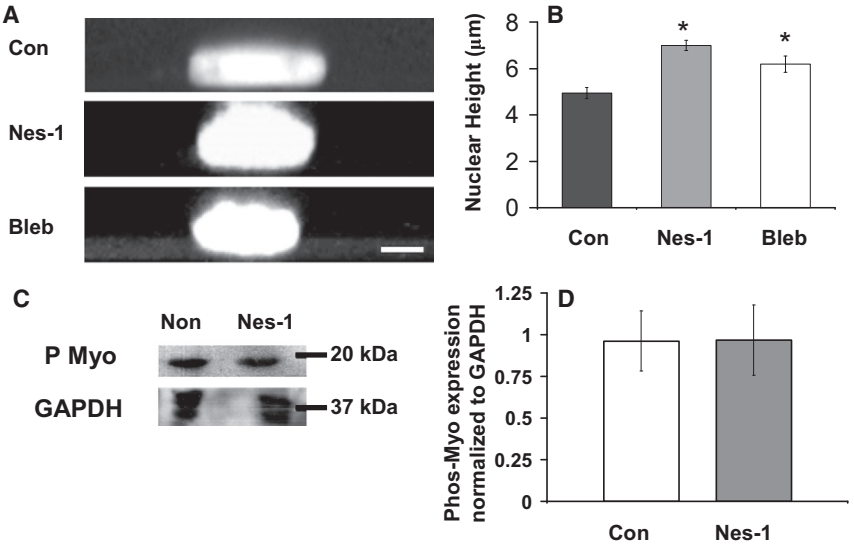

FIGURE 5 Nuclear height increases in nesprin-1 deficient HUVECs. (*A*) Representative Z-stack images generated with confocal microscopy show an increase in nuclear height in nesprin-1 deficient and blebbistatin (bleb)-treated cells. Hoechst33342 was used to stain the nucleus. Scale bar = 5 μm. (*B*) Plot quantifies the increase in nuclear height of nesprin-1 deficient HUVECs and HUVECs treated with blebbistatin. Error bars represent SE; $*p < 0.05$ (each statistical comparison is with Con). A minimum of 15 cells were measured for each condition. (*C*) Western blot of phosphorylated myosin (P Myo) in nontransfected and siRNA transfected cells. (*D*) Quantification shows no difference in myosin II light chain phosphorylation. Error bars represent SE from three different experiments.

The increase in nuclear height in nesprin-1 depleted cells observed above could be attributed potentially to differences in nonmuscle myosin II activity. However, Western blotting showed that the levels of phosphorylated nonmuscle myosin II are unchanged in nesprin-1 depleted cells compared to control (Fig. 5, *C* and *D*).

Nesprin-1 deficiency causes abnormal HUVEC migration

Increased traction and focal adhesions typically correlate with a decrease in cell migration speed (38,39). We therefore tested whether nesprin-1 depletion alters cell migration in a scratch-wound assay. Time lapse imaging over the course of 12 h was carried out on wounded monolayers of nesprin-1 depleted and control cells. Cells transfected with control siRNA completely closed the scratched wound in around 8 h (Fig. 6 and Movie S1). In contrast, cells transfected with nesprin-1 targeting siRNA failed to close the wound at 8 h (Fig. 6 and Movie S2).

To examine if nesprin-1 deficiency also affects individual cell motility, migrating cells were imaged with phase contrast microscopy, and the time-dependent position of the nuclear centroid was quantified. MSD data were calculated

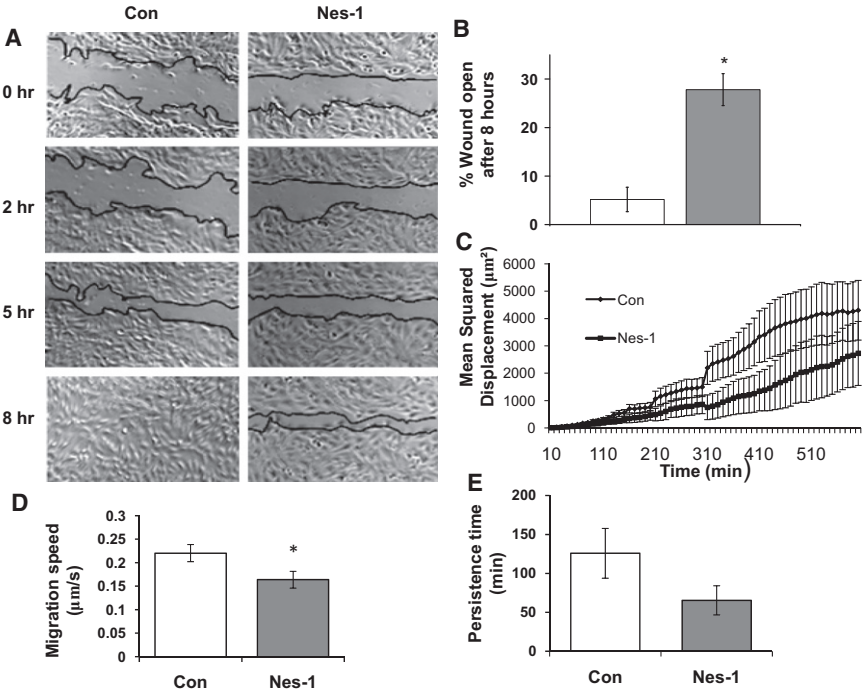

FIGURE 6 Nesprin-1 deficient HUVECs have decreased wound healing rates, single-cell speed, and persistence times. (*A*) Phase contrast images of HUVECs at 0, 2, 5, and 8 h after wounding are shown. Wound edges are marked in black. Scale bar = 200 μm. (*B*) Plot shows the unhealed percentage of the original wound for HUVECs transfected with control and nesprin-1 siRNA at 8 h. Error bars represent SE from three different experiments. $*p < 0.01$. (*C*) Plot shows MSD calculated using single-cell trajectories and pooled together from at least 10 different cells. Error bars represent SE. MSD is decreased significantly in nesprin-1 deficient cells. (*D*) Individual cell migration speed, and (*E*) persistence time is decreased in nesprin-1 deficient cells; the decrease in persistence time is not statistically significant. At least 17 cells were analyzed for each condition in the motility experiments. $*p < 0.05$.

with nonoverlapping intervals and fit to a model for cell migration. We found that the speed of single cells was significantly decreased in nesprin-1 deficient cells compared to control (Fig. 6 *D*).

DISCUSSION

The mechanical linkage between the nucleus and the actomyosin cytoskeleton was demonstrated several years ago by showing that applied force to transmembrane integrins at the endothelial cell membrane caused deformation of the nucleus (35). Actomyosin tension exerted on the nucleus has been shown to stabilize its shape (34). This linkage is also crucial for the cell's ability to position the nucleus in the cell (4). The recent discovery of LINC complex proteins has triggered interest in the function of specific molecular linkers in nucleo-cytoskeletal force transfer. In this study, we provide evidence for new functions of nesprin-1, a nuclear membrane protein that links the nucleus to the F-actin cytoskeleton. Nesprin-1 depletion causes abnormal cell reorientation under cyclic strain, increased nuclear height, decreased cell migration, and increased adhesion assembly and traction in endothelial cells.

In the absence of nesprin-1, we found that cells are unable to reorient in response to uniaxial cyclic strain; however, transient disassembly of adhesions restores HUVEC reorientation. It is known that elevation of actomyosin tension causes increased cell-substrate adhesion that interferes with cellular reorientation under applied strain (33). However, we did not find any differences in myosin phosphorylation (that typically correlates with actomyosin tension (27)) in nesprin-1 deficient cells or in microtubule and intermediate filament organization (Fig. S9). Yet, we found that nesprin-1 deficient cells assemble more focal adhesions, have more concentrated F-actin toward the base of the cell and exert more traction on the substrate compared to control cells. Nesprin-1 deficient cells also had increased nuclear heights similar to cells with inhibited myosin activity suggesting that nesprin-1 may decouple tensile actomyosin forces from the nucleus.

To explain these findings, we propose a model (Fig. 7) in which part of the actomyosin tension is exerted on (and balanced by) the nucleus through connections mediated by nesprin-1. In the absence of these connections, the actomyosin forces are assumed to be balanced at an additional number of focal adhesions, which will result in greater traction stresses on the substrate. A key feature of the model is that increased substrate deformation can result even though myosin activity is unchanged. Increased focal adhesion assembly and traction stresses would then prevent cell reorientation under cyclic strain, in a similar manner to cells with increased actomyosin tension (33). Additionally, as actomyosin forces are redirected from the nucleus to the substrate due to the lack of nesprin-1 mediated binding, less actomyosin tension is exerted on the nucleus. This

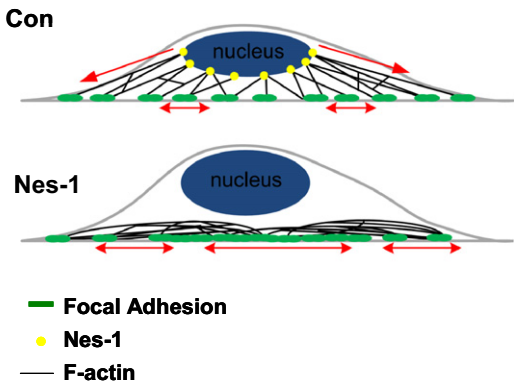

FIGURE 7 Physical model for nuclear-actomyosin force balance. In control cells (*top*) the actomyosin tension is balanced in part by the nucleus due to mechanical links mediated by nesprin-1. In the absence of nesprin-1 (*bottom*), the forces are balanced by the substrate at an increased number of focal adhesions even though myosin II activity is unchanged.

tension (that would normally balance osmotic pressure (34)) is decreased, resulting in increased nuclear height.

The observed decrease in cell migration speed is consistent with increased adhesion assembly and traction. This is because cell speed is low at low and high adhesive strengths, and is maximum at an intermediate value (38,40,41). As the nesprin-1 depleted cells form more focal adhesions than normal cells(Fig. 3, *A* and *B*), cell migration speed is expected to decrease (Fig. 6 *D*).

Whereas the model in Fig. 7 is consistent with our observations, it is a static model that does not offer an explanation of how more focal adhesions are formed when actomyosin is disconnected from the nuclear surface. Future studies that investigate the dynamic assembly and disassembly of adhesions, and the fate of rearward actomyosin flow from the membrane in nesprin-1 deficient cells could help better answer this question. Other nesprin isoforms such as nesprin-2 also link the nuclear surface to the actomyosin cytoskeleton (13,16,20,42) and could possibly compensate for nesprin-1 (16). However, the fact that nesprin-2 expression (Fig. S2, *A* and *B*) and localization (Fig. S3) was not altered by nesprin-1 knockdown, and yet F-actin distribution was perturbed (Fig. S6) suggests that nesprin-1 may play an essential role in linking the nucleus and F-actin.

In summary, our results suggest an important role for nesprin-1 in endothelial cell function. In the absence of nesprin-1, endothelial cells assemble more adhesions, exert greater traction on the surface, have increased nuclear heights, and have decreased migration speeds. Nonmuscle myosin II phosphorylation is unchanged in nesprin-1 depleted cells. These results support a model in which actomyosin tension normally balanced by the nucleus is balanced in nesprin-1 deficient cells by the substrate. Our findings with nesprin-1 depleted cells show a remarkable similarity with other recent studies that have shown decreased speeds of wound healing and defective nuclear positioning in lamin A/C and emerin deficient cells (5,7). Given that lamin A/C and emerin are

structurally and functionally different from nesprin-1, this raises the possibility that other LINC complex proteins may also influence cell behavior in a manner similar to the proposed model.

SUPPORTING MATERIAL

Two movies and three figures are available at http://www.biophysj.org/biophysj/supplemental/S0006-3495(10)00470-4.

This work was supported by the American Heart Association (0735203N to T.P.L., 0635095N to C.K.T.) and the National Science Foundation (00072397 to T.P.L.).

REFERENCES

1. Huang, S., and D. E. Ingber. 1999. The structural and mechanical complexity of cell-growth control. *Nat. Cell Biol.* 1:E131–E138.
2. Lauffenburger, D. A., and A. F. Horwitz. 1996. Cell migration: a physically integrated molecular process. *Cell.* 84:359–369.
3. Ferrara, N., H. P. Gerber, and J. LeCouter. 2003. The biology of VEGF and its receptors. *Nat. Med.* 9:669–676.
4. Starr, D. A. 2009. A nuclear-envelope bridge positions nuclei and moves chromosomes. *J. Cell Sci.* 122:577–586.
5. Hale, C. M., A. L. Shrestha, …, D. Wirtz. 2008. Dysfunctional connections between the nucleus and the actin and microtubule networks in laminopathic models. *Biophys. J.* 95:5462–5475.
6. Lammerding, J., P. C. Schulze, …, R. T. Lee. 2004. Lamin A/C deficiency causes defective nuclear mechanics and mechanotransduction. *J. Clin. Invest.* 113:370–378.
7. Lee, J. S., C. M. Hale, …, D. Wirtz. 2007. Nuclear lamin A/C deficiency induces defects in cell mechanics, polarization, and migration. *Biophys. J.* 93:2542–2552.
8. Haque, F., D. J. Lloyd, …, S. Shackleton. 2006. SUN1 interacts with nuclear lamin A and cytoplasmic nesprins to provide a physical connection between the nuclear lamina and the cytoskeleton. *Mol. Cell. Biol.* 26:3738–3751.
9. Worman, H. J., and G. G. Gundersen. 2006. Here come the SUNs: a nucleocytoskeletal missing link. *Trends Cell Biol.* 16:67–69.
10. Padmakumar, V. C., T. Libotte, …, I. Karakesisoglou. 2005. The inner nuclear membrane protein Sun1 mediates the anchorage of Nesprin-2 to the nuclear envelope. *J. Cell Sci.* 118:3419–3430.
11. Starr, D. A., and M. Han. 2002. Role of ANC-1 in tethering nuclei to the actin cytoskeleton. *Science.* 298:406–409.
12. Lammerding, J., J. Hsiao, …, R. T. Lee. 2005. Abnormal nuclear shape and impaired mechanotransduction in emerin-deficient cells. *J. Cell Biol.* 170:781–791.
13. Zhang, Q., C. Bethmann, …, C. M. Shanahan. 2007. Nesprin-1 and -2 are involved in the pathogenesis of Emery Dreifuss muscular dystrophy and are critical for nuclear envelope integrity. *Hum. Mol. Genet.* 16:2816–2833.
14. Mislow, J. M., J. M. Holaska, …, E. M. McNally. 2002. Nesprin-1alpha self-associates and binds directly to emerin and lamin A in vitro. *FEBS Lett.* 525:135–140.
15. Roux, K. J., M. L. Crisp, …, B. Burke. 2009. Nesprin 4 is an outer nuclear membrane protein that can induce kinesin-mediated cell polarization. *Proc. Natl. Acad. Sci. USA.* 106:2194–2199.
16. Zhang, X., R. Xu, …, M. Han. 2007. Syne-1 and Syne-2 play crucial roles in myonuclear anchorage and motor neuron innervation. *Development.* 134:901–908.
17. Broers, J. L., E. A. Peeters, …, F. C. Ramaekers. 2004. Decreased mechanical stiffness in LMNA-/- cells is caused by defective nucleocytoskeletal integrity: implications for the development of laminopathies. *Hum. Mol. Genet.* 13:2567–2580.
18. Stewart-Hutchinson, P. J., C. M. Hale, …, D. Hodzic. 2008. Structural requirements for the assembly of LINC complexes and their function in cellular mechanical stiffness. *Exp. Cell Res.* 314:1892–1905.
19. Zhang, Q., C. Ragnauth, …, R. G. Roberts. 2002. The nesprins are giant actin-binding proteins, orthologous to *Drosophila melanogaster* muscle protein MSP-300. *Genomics.* 80:473–481.
20. Crisp, M., Q. Liu, …, D. Hodzic. 2006. Coupling of the nucleus and cytoplasm: role of the LINC complex. *J. Cell Biol.* 172:41–53.
21. Zhang, Q., J. N. Skepper, …, C. M. Shanahan. 2001. Nesprins: a novel family of spectrin-repeat-containing proteins that localize to the nuclear membrane in multiple tissues. *J. Cell Sci.* 114:4485–4498.
22. Grady, R. M., D. A. Starr, …, M. Han. 2005. Syne proteins anchor muscle nuclei at the neuromuscular junction. *Proc. Natl. Acad. Sci. USA.* 102:4359–4364.
23. Puckelwartz, M. J., E. Kessler, …, E. M. McNally. 2009. Disruption of nesprin-1 produces an Emery Dreifuss muscular dystrophy-like phenotype in mice. *Hum. Mol. Genet.* 18:607–620.
24. Thodeti, C. K., B. Matthews, …, D. E. Ingber. 2009. TRPV4 channels mediate cyclic strain-induced endothelial cell reorientation through integrin-to-integrin signaling. *Circ. Res.* 104:1123–1130.
25. Dickinson, R. B., and R. T. Tranquillo. 1993. A stochastic model for adhesion-mediated cell random motility and haptotaxis. *J. Math. Biol.* 31:563–600.
26. Harms, B. D., G. M. Bassi, …, D. A. Lauffenburger. 2005. Directional persistence of EGF-induced cell migration is associated with stabilization of lamellipodial protrusions. *Biophys. J.* 88:1479–1488.
27. Polte, T. R., G. S. Eichler, …, D. E. Ingber. 2004. Extracellular matrix controls myosin light chain phosphorylation and cell contractility through modulation of cell shape and cytoskeletal prestress. *Am. J. Physiol. Cell Physiol.* 286:C518–C528.
28. Tolić-Nørrelykke, I. M., J. P. Butler, …, N. Wang. 2002. Spatial and temporal traction response in human airway smooth muscle cells. *Am. J. Physiol. Cell Physiol.* 283:C1254–C1266.
29. Mislow, J. M., M. S. Kim, …, E. M. McNally. 2002. Myne-1, a spectrin repeat transmembrane protein of the myocyte inner nuclear membrane, interacts with lamin A/C. *J. Cell Sci.* 115:61–70.
30. Padmakumar, V. C., S. Abraham, …, E. Korenbaum. 2004. Enaptin, a giant actin-binding protein, is an element of the nuclear membrane and the actin cytoskeleton. *Exp. Cell Res.* 295:330–339.
31. Hayakawa, K., N. Sato, and T. Obinata. 2001. Dynamic reorientation of cultured cells and stress fibers under mechanical stress from periodic stretching. *Exp. Cell Res.* 268:104–114.
32. Lele, T. P., J. Pendse, …, D. E. Ingber. 2006. Mechanical forces alter zyxin unbinding kinetics within focal adhesions of living cells. *J. Cell. Physiol.* 207:187–194.
33. Ghosh, K., C. K. Thodeti, …, D. E. Ingber. 2008. Tumor-derived endothelial cells exhibit aberrant Rho-mediated mechanosensing and abnormal angiogenesis in vitro. *Proc. Natl. Acad. Sci. USA.* 105: 11305–11310.
34. Sims, J. R., S. Karp, and D. E. Ingber. 1992. Altering the cellular mechanical force balance results in integrated changes in cell, cytoskeletal and nuclear shape. *J. Cell Sci.* 103:1215–1222.
35. Maniotis, A. J., C. S. Chen, and D. E. Ingber. 1997. Demonstration of mechanical connections between integrins, cytoskeletal filaments, and nucleoplasm that stabilize nuclear structure. *Proc. Natl. Acad. Sci. USA.* 94:849–854.
36. Hu, S., J. Chen, …, N. Wang. 2005. Prestress mediates force propagation into the nucleus. *Biochem. Biophys. Res. Commun.* 329:423–428.
37. Gomes, E. R., S. Jani, and G. G. Gundersen. 2005. Nuclear movement regulated by Cdc42, MRCK, myosin, and actin flow establishes MTOC polarization in migrating cells. *Cell.* 121:451–463.
38. Palecek, S. P., J. C. Loftus, …, A. F. Horwitz. 1997. Integrin-ligand binding properties govern cell migration speed through cell-substratum adhesiveness. *Nature.* 385:537–540.

39. Pelham, Jr., R. J., and Y. Wang. 1997. Cell locomotion and focal adhesions are regulated by substrate flexibility. *Proc. Natl. Acad. Sci. USA*. 94:13661–13665.

40. Burgess, B. T., J. L. Myles, and R. B. Dickinson. 2000. Quantitative analysis of adhesion-mediated cell migration in three-dimensional gels of RGD-grafted collagen. *Ann. Biomed. Eng*. 28:110–118.

41. Peyton, S. R., and A. J. Putnam. 2005. Extracellular matrix rigidity governs smooth muscle cell motility in a biphasic fashion. *J. Cell. Physiol.* 204:198–209.

42. Libotte, T., H. Zaim, …, I. Karakesisoglou. 2005. Lamin A/C-dependent localization of Nesprin-2, a giant scaffolder at the nuclear envelope. *Mol. Biol. Cell.* 16:3411–3424.